

Role for integrin-linked kinase in mediating tubular epithelial to mesenchymal transition and renal interstitial fibrogenesis

Yingjian Li, Junwei Yang, Chunsun Dai, Chuanyue Wu, and Youhua Liu

Department of Pathology, University of Pittsburgh School of Medicine, Pittsburgh, Pennsylvania, USA

Under pathologic conditions, renal tubular epithelial cells can undergo epithelial to mesenchymal transition (EMT), a phenotypic conversion that is believed to play a critical role in renal interstitial fibrogenesis. However, the underlying mechanism that governs this process remains largely unknown. Here we demonstrate that integrin-linked kinase (ILK) plays an important role in mediating tubular EMT induced by TGF- β 1. TGF- β 1 induced ILK expression in renal tubular epithelial cells in a time- and dose-dependent manner, which was dependent on intracellular Smad signaling. Forced expression of ILK in human kidney proximal tubular epithelial cells suppressed E-cadherin expression and induced fibronectin expression and its extracellular assembly. ILK also induced MMP-2 expression and promoted cell migration and invasion in Matrigel. Conversely, ectopic expression of a dominant-negative, kinase-dead form of ILK largely abrogated TGF- β 1-initiated tubular cell phenotypic conversion. In vivo, ILK was markedly induced in renal tubular epithelia in mouse models of chronic renal diseases, and such induction was spatially and temporally correlated with tubular EMT. Moreover, inhibition of ILK expression by HGF was associated with blockade of tubular EMT and attenuation of renal fibrosis. These findings suggest that ILK is a critical mediator for tubular EMT and likely plays a crucial role in the pathogenesis of chronic renal fibrosis.

J. Clin. Invest. 112:503–516 (2003). doi:10.1172/JCI200317913.

Introduction

Emerging evidence suggests that renal tubular epithelial cells can undergo epithelial to mesenchymal transition (EMT) to become matrix-producing fibroblasts under pathologic conditions (1, 2). This phenotypic conversion not only illustrates the remarkable plasticity of mature, differentiated kidney epithelial cells, but is also fundamentally implicated in the pathogenesis of a wide range of chronic renal diseases (3–6). Recent studies provide compelling evidence that a large proportion of the interstitial fibroblasts in fibrotic kidneys originate from tubular epithelial cells via EMT (3). Likewise, selective blockade of tubular EMT, due to preservation of tubular basement membrane (TBM) integrity in *tPA*^{-/-} mice, protects the kidney from developing fibrotic lesions after obstructive injury (4). These observations underscore the crucial importance of tubular EMT in the onset and pro-

gression of chronic renal fibrosis that eventually results in end-stage renal failure.

Tubular EMT is regulated by numerous growth factors and hormones in different ways (2, 6–10). TGF- β 1 is perhaps the principal factor that promotes EMT in vitro. Earlier studies indicate that TGF- β 1 as a sole factor initiates and completes the entire EMT course that consists of four key steps (2). Given the well-documented profibrotic activity of TGF- β 1 (11–14), it is conceivable that the ability to initiate tubular EMT may play a pivotal role in mediating TGF- β 1's actions. In accordance with this, both TGF- β 1 and its type I receptor are found to be specifically upregulated in renal tubular epithelia after chronic injury (6, 15), suggesting that tubular epithelial cells are the natural targets of this fibrotic cytokine in a pathologic setting. In vitro, TGF- β 1 orchestrates sequential cellular events that include loss of epithelial adhesion, F-actin reorganization, disruption of TBM integrity, and enhanced cell migration and invasion (2, 8, 9). However, the underlying mechanism by which TGF- β 1 initiates this mesenchymal transition of tubular epithelial cells remains largely unknown.

Integrin-linked kinase (ILK) is an intracellular serine/threonine protein kinase that interacts with the cytoplasmic domains of β -integrins and numerous cytoskeleton-associated proteins (16–19). ILK has been shown to be involved in the regulation of a number of integrin-mediated processes that include cell adhesion, cell shape changes, gene expression, and ECM deposition (20). Recent studies have implicated

Received for publication January 20, 2003, and accepted in revised form June 10, 2003.

Address correspondence to: Youhua Liu, Department of Pathology, University of Pittsburgh School of Medicine, S-405 Biomedical Science Tower, 200 Lothrop Street, Pittsburgh, Pennsylvania 15261, USA. Phone: (412) 648-8253; Fax: (412) 648-1916; E-mail: liuy@msx.upmc.edu. Yingjian Li and Junwei Yang contributed equally to this work.

Conflict of interest: The authors have declared that no conflict of interest exists.

Nonstandard abbreviations used: epithelial to mesenchymal transition (EMT); tubular basement membrane (TBM); integrin-linked kinase (ILK); kinase-dead ILK (kd-ILK); protein kinase A (PKA); unilateral ureteral obstruction (UUO).

ILK dysregulation in the development of several chronic glomerular diseases. For instance, using an unbiased mRNA expression screening approach, Kretzler et al. identified ILK as a candidate downstream effector in proteinuria in patients with congenital nephritic syndrome (21). Overexpression of ILK is also observed in glomerular podocytes in two murine proteinuria models. Such alteration in ILK abundance is associated with progressive focal segmental glomerulosclerosis (21). Likewise, analyses of glomerular mesangial cells and human kidney tissues suggest that ILK is involved in mesangial matrix expansion in response to hyperglycemia in diabetic nephropathy (22). However, questions remain as to whether dysregulation of ILK is also implicated in chronic renal interstitial fibrosis, and if so, how ILK induction leads to activation of matrix-producing fibroblasts, the cells principally responsible for excess production of ECM in the fibrotic kidney.

In this study, we demonstrate that ILK expression is specifically induced in renal tubular epithelial cells in response to TGF- β 1 treatment in vitro and after obstructive or diabetic injury in vivo. Ectopic expression of ILK suppresses expression of the epithelial marker E-cadherin and induces expression of the interstitial matrix component fibronectin and its extracellular assembly. Consistently, overexpression of kinase-dead ILK (kd-ILK) largely abolishes TGF- β 1-induced mesenchymal transition of tubular epithelial cells. Our observations suggest a crucial role for ILK in mediating TGF- β 1-induced tubular EMT.

Methods

Ab's, plasmids, and reagents. The rabbit polyclonal anti-ILK Ab was purchased from Upstate Biotechnology Inc. (Charlottesville, Virginia, USA) and used for Western blot. The mouse monoclonal anti-ILK Ab was described previously (22) and was used for immunofluorescence staining. The mouse monoclonal Ab's against E-cadherin (clone 36) and fibronectin (clone 10) were purchased from BD Pharmingen (San Jose, California, USA). The phosphospecific Smad-2 Ab and total Smad-2 Ab were purchased from Upstate Biotechnology Inc. The Ab's against phosphospecific and total Akt kinase, and phosphospecific and total p38 MAPK, were obtained from Cell Signaling Technology Inc. (Beverly, Massachusetts, USA). The anti-Smad-7 (sc-7004), anti-Snail (sc-10433), and anti-actin (sc-1616) Ab's were purchased from Santa Cruz Biotechnology Inc. (Santa Cruz, California, USA). The anti-human MMP-2 Ab (AB809) was obtained from Chemicon International (Temecula, California, USA). The anti- α -smooth muscle actin (clone 1A4) was purchased from Sigma-Aldrich (St. Louis, Missouri, USA). Affinity-purified secondary Ab's were purchased from Jackson ImmunoResearch Laboratories Inc. (West Grove, Pennsylvania, USA). The eukaryotic expression plasmid (pCMV-WT-ILK) containing

WT human ILK cDNA under the control of the CMV promoter, the kd-ILK expression vector pCMV-kd-ILK, and empty vector (pUSEamp) were obtained from Upstate Biotechnology Inc. The kd-ILK vector contains a single-point mutation by substitution of G for A at nucleotide 1,075 of the ILK cDNA. The Smad-7 expression vector containing mouse Smad-7 cDNA under the control of the CMV promoter was provided by P. ten Dijke of the Ludwig Institute for Cancer Research (Uppsala, Sweden) (23). The Snail expression vector (pHA-Snail) was generously provided by A. Garcia de Herreros of Universitat Pompeu Fabra (Barcelona, Spain) (24). The empty pcDNA3 vector was purchased from Invitrogen Corp. (Carlsbad, California, USA). Recombinant human TGF- β 1 was purchased from R&D Systems Inc. (Minneapolis, Minnesota, USA). Recombinant human HGF was provided by Genentech Inc. (South San Francisco, California, USA). Cell culture media, FBS, and supplements were obtained from Invitrogen Corp. Mek1 inhibitor PD98059, the PI3K inhibitor wortmannin, myristoylated protein kinase A (PKA) inhibitor, the PKC inhibitor Ro-31-8220, and p38 MAPK inhibitor SC68376 were purchased from Calbiochem-Novabiochem Corp. (La Jolla, California, USA). All other chemicals were of analytic grade and were obtained from Sigma-Aldrich or Fisher Scientific Co. (Pittsburgh, Pennsylvania, USA) unless otherwise indicated.

Cell culture and treatment. Human kidney proximal tubular epithelial cell line (HKC) was provided by L. Racusen of Johns Hopkins University (Baltimore, Maryland, USA) (25). Cells were cultured in DMEM/Ham's F12 medium supplemented with 10% FBS. HKC cells were seeded at approximately 70% confluence in complete medium containing 10% FBS. Twenty-four hours later, the cells were changed to serum-free medium and incubated for 16 hours. Cells were then treated with recombinant TGF- β 1 for various periods of time as indicated. The cells were then collected at different timepoints for Western blot analysis and immunofluorescence staining. In some experiments, cells were pretreated for 30 minutes with various chemical inhibitors at the concentrations specified, followed by incubating in the absence or presence of 2 ng/ml of TGF- β 1.

Establishment of stable cell lines. HKC cells were transfected with various expression plasmids containing either WT human ILK cDNA (pCMV-WT-ILK) or kd-ILK cDNA (pCMV-kd-ILK), respectively, using Lipofectamine 2000 (Invitrogen Corp.) according to the instructions specified by the manufacturer. The empty vector pUSEamp (Upstate Biotechnology Inc.) was used as a mock-transfection control. Twenty-four hours after transfection and every 3–4 days thereafter, the cells were re-fed with fresh selective medium containing G418 (geneticin; Invitrogen Corp.) at a final concentration of 800 μ g/ml (26). Neomycin-resistant clones were first visible after 7 days and continuously

cultured in selective medium for about 14 days. The cell clones were then individually transferred into six-well plates for expansion using a cloning cylinder (Sigma-Aldrich). After two further passages in selective medium, expanded independent clones were cultured in standard medium. Ectopic expression of WT or kd ILK in the stable cell lines was confirmed by Western blot analysis. The stable cell line overexpressing Smad-7 (HKC^{Smad7}) and the corresponding control cell line (HKC^{pcDNA3}) were established as described previously (27).

Animal model. Male CD-1 mice weighing 20–22 g were obtained from Harlan Sprague Dawley Inc. (Indianapolis, Indiana, USA). Unilateral ureteral obstruction (UUO) was performed using an established procedure as described elsewhere (10, 28, 29). Administration of HGF into mice was performed as described previously (6). Briefly, starting the day of surgery, mice were injected with recombinant human HGF through the tail vein at a dose of 200 µg/kg body weight every 12 hours for 6 days. Control mice were injected with the same volume of vehicle (0.9% saline solution). Mice were sacrificed at different timepoints as indicated after surgery, and kidneys were removed. One part of the kidneys was fixed in 10% phosphate-buffered formalin, followed by paraffin embedding for histologic and immunohistochemical studies. Another part was immediately frozen in Tissue-Tek OCT compound (Sakura Finetek Inc., Torrance, California, USA) for cryosection. The remaining kidneys were snap-frozen in liquid nitrogen and stored at -80°C for protein extractions.

To study ILK expression in another model of chronic renal disease, a uninephrectomized diabetic mouse model was used. It has been shown that this model exhibits an accelerated progression of diabetic nephropathy (30). Briefly, male CD-1 mice underwent uninephrectomy 1 week prior to intravenous injection of streptozotocin at 150 mg/kg body weight. A group of mice that underwent sham operation and received no streptozotocin injection served as normal control. Three months after injection of streptozotocin, mice were sacrificed and kidney morphology and function and renal ILK expression were respectively analyzed.

Western blot analysis. Cell lysates and kidney tissue homogenates were prepared as described previously (10). Samples were heated at 100°C for approximately 5–10 minutes before loading and separated on precast 10% SDS-polyacrylamide gels (Bio-Rad Laboratories Inc., Hercules, California, USA). After the proteins were electrotransferred to a nitrocellulose membrane (Amersham Biosciences, Piscataway, New Jersey, USA), non-specific binding to the membrane was blocked for 1 hour at room temperature with 5% Carnation nonfat milk in TBS buffer (20 mM Tris-HCl, 150 mM NaCl, and 0.1% Tween 20). The membranes were then incubated for 16 hours at 4°C with various primary Ab's in blocking buffer containing 5% milk at the dilutions specified by the manufacturers. Following extensive

washing in TBS buffer, the membranes were incubated with HRP-conjugated secondary Ab for 1 hour at room temperature in 5% nonfat milk dissolved in TBS. Membranes were then washed with TBS buffer and the signals were visualized using the ECL system (Amersham Biosciences) as described previously (6).

Immunofluorescence staining. Indirect immunofluorescence staining was performed using an established procedure (6). Briefly, cells cultured on coverslips were washed twice with cold PBS and fixed with cold methanol/acetone (1:1) for 10 minutes at -20°C. Following three extensive washings with PBS containing 0.5% BSA, the cells were blocked with 20% normal donkey serum in PBS buffer for 30 minutes at room temperature and then incubated with the specific primary Ab's described above. Kidney cryosections were prepared at 5 µm thickness and fixed for 10 minutes with cold methanol/acetone (1:1). After being blocked with 20% normal donkey serum in PBS for 30 minutes, the sections were incubated with anti-ILK or anti-α-smooth muscle actin Ab's. As a negative control, the primary Ab was replaced with non-immune IgG, and no staining occurred. Kidney cryosections were also stained with a renal proximal tubular marker, fluorescein-conjugated lectin from *Tetragonolobus purpureas* (Sigma-Aldrich). For some samples, cells were double stained with DAPI to visualize the nuclei. Stained cells and cryosections were mounted with Vectashield mounting medium (Vector Laboratories Inc., Burlingame, California, USA) and viewed with a Nikon Eclipse E600 epifluorescence microscope equipped with a digital camera (Nikon Inc., Melville, New York, USA).

Northern blot analysis. Total RNA was extracted from various cell lines and the kidney tissue using an Ultraspec RNA isolation system according to the instructions specified by the manufacturer (Biotecx Laboratories Inc., Houston, Texas, USA) (31). Northern blot analysis for gene expression was carried out by the procedures described previously (4). Briefly, samples of 20 µg total RNA were electrophoresed on 1.0% formaldehyde-agarose gels and then transferred to GeneScreen Plus nylon membrane (PerkinElmer Inc., Boston, Massachusetts, USA) by capillary blotting. Membranes were prehybridized and hybridized at 65°C for 4 hours and 16 hours, respectively. ³²P-labeled DNA probes were prepared using a random primer labeling kit (Stratagene, La Jolla, California, USA) using [α-³²P]dCTP. After autoradiography, membranes were stripped and rehybridized with rat GAPDH probe to assure equal loading of each lane.

Biochemical determination of fibronectin assembly. The extracellular assembly of fibronectin was quantitatively determined by a biochemical method as described previously by Wu et al. (20). Briefly, 3 × 10⁶ cells were seeded in 100-mm tissue culture plates in complete medium as described above and incubated for 2 days. The cell monolayers were then washed three times with PBS containing 1 mM 4-(2-

aminoethyl)benzenesulfonylfluoride (AEBSF) and harvested with a rubber policeman. The ECM fraction was isolated by sequential extraction of the cells with (a) 3% Triton X-100 in PBS containing 1 mM AEBSF; (b) 100 μ g/ml DNase I in 50 mM Tris, pH 7.4, 10 mM MnCl₂, 1 M NaCl, and 1 mM AEBSF; and (c) 2% deoxycholate in Tris, pH 8.8, and 1 mM AEBSF. Fibronectin in the deoxycholate-insoluble ECM fraction was analyzed by Western blot with monoclonal anti-fibronectin Ab according to the method described above.

Gelatin zymographic analysis. Zymographic analysis of MMP proteolytic activity in the supernatant of cultured cells was performed according to the method described previously (2). Briefly, a constant amount of protein from the conditioned media (15 μ g) was loaded into 10% SDS-polyacrylamide gel containing 1 mg/ml gelatin (Bio-Rad Laboratories Inc.). After electrophoresis, SDS was removed from the gel by incubation in 2.5% Triton X-100 at room temperature for 30 minutes with gentle shaking. The gel was washed well with distilled water and incubated at 37°C for 16–36 hours in a developing buffer containing 50 mM Tris-HCl, pH 7.6, 0.2 M NaCl, 5 mM CaCl₂, and 0.02% Brij 35. The gel was then stained with a solution of 30% methanol, 10% glacial acetic acid, and 0.5% Coomassie blue G250, followed by destaining in the same solution without dye. Proteinase activity was detected as unstained bands on a blue background representing areas of gelatin digestion.

Boyden chamber motility assay. Cell migration was evaluated using a Boyden chamber motility assay with tissue culture-treated Transwell filters (Corn-

ing-Costar Corp., Corning, New York, USA) (2). Cells (1×10^4) were seeded onto the filters (8 μ m pore size, 0.33 cm² growth area) in the top compartment of the chamber. After 5 days of incubation at 37°C, filters were fixed with 3% paraformaldehyde in PBS and stained with 0.1% Coomassie blue in 10% methanol and 10% acetic acid, and the upper surface of the filters was carefully wiped with a cotton-tipped applicator. Cells and cell extensions that passed through the pores were counted in five nonoverlapping $\times 20$ fields and photographed under a Nikon microscope.

Matrigel invasion assay. Matrigel (1.43 mg/cm²) (BD Biosciences, San Jose, California, USA) was added to the Transwell filters (8 μ m pore size, 0.33 cm² growth area) of a Boyden chamber to form matrix gels at 1.0 mm depth (2). Cells (1×10^4) in a volume of 100 μ l were added to the top of the gels. After 5 days of incubation at 37°C, filters were fixed with 3% paraformaldehyde in PBS and stained with 0.1% Coomassie blue in 10% methanol and 10% acetic acid, and the upper surface of the filters was carefully wiped with a cotton-tipped applicator. Cell extensions that invaded and migrated across the Matrigel and passed through the Transwell filter pores toward the lower surface of the filters were counted in five nonoverlapping $\times 10$ fields. The experiments were carried out in triplicate cultures.

Statistical analysis. Statistical analysis of the data was performed using SigmaStat software (Jandel Scientific Software, San Rafael, California, USA). Comparison between groups was made using one-way

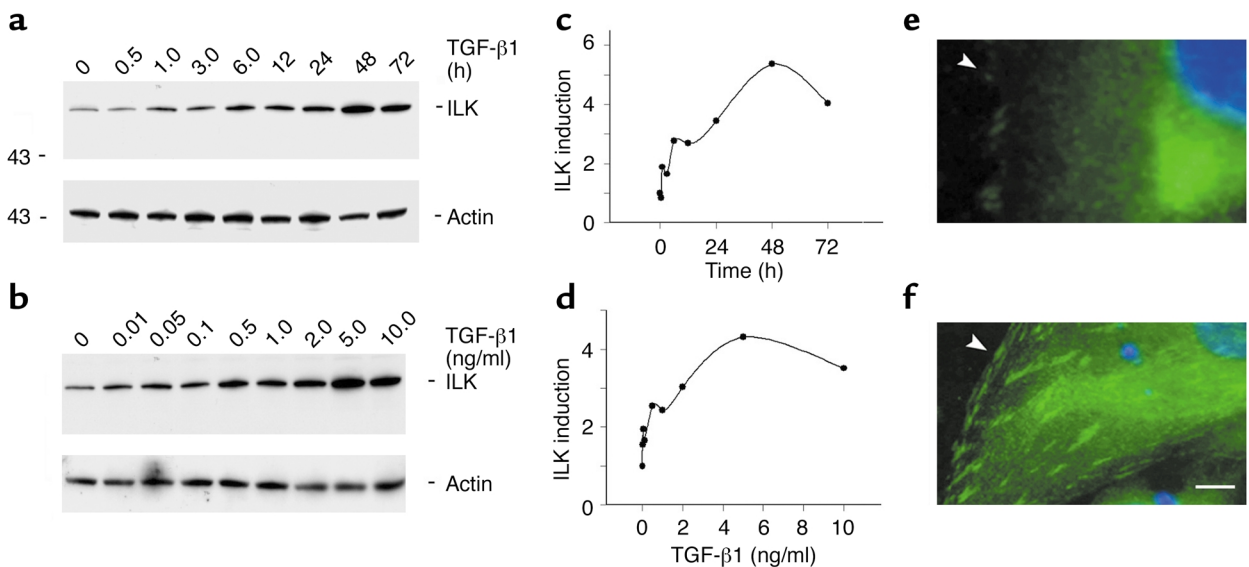


Figure 1

TGF- β 1 induces ILK expression in renal tubular epithelial cells. (a–d) Western blot analyses show that TGF- β 1 induced ILK protein expression in a time- and dose-dependent manner. HKC cells were incubated with either the same concentration of TGF- β 1 (2 ng/ml) for various periods of time (a and c) or with increasing amounts of TGF- β 1 for 24 hours (b and d). Cell lysates were immunoblotted with Ab's against ILK and actin, respectively. (c and d) Graphic presentation of relative ILK abundance (fold induction) normalized to actin. (e and f) Immunofluorescence staining shows the localization of ILK in control (e) or TGF- β 1-treated HKC cells (f). Arrowheads indicate positive ILK staining. Scale bar, 5 μ m.

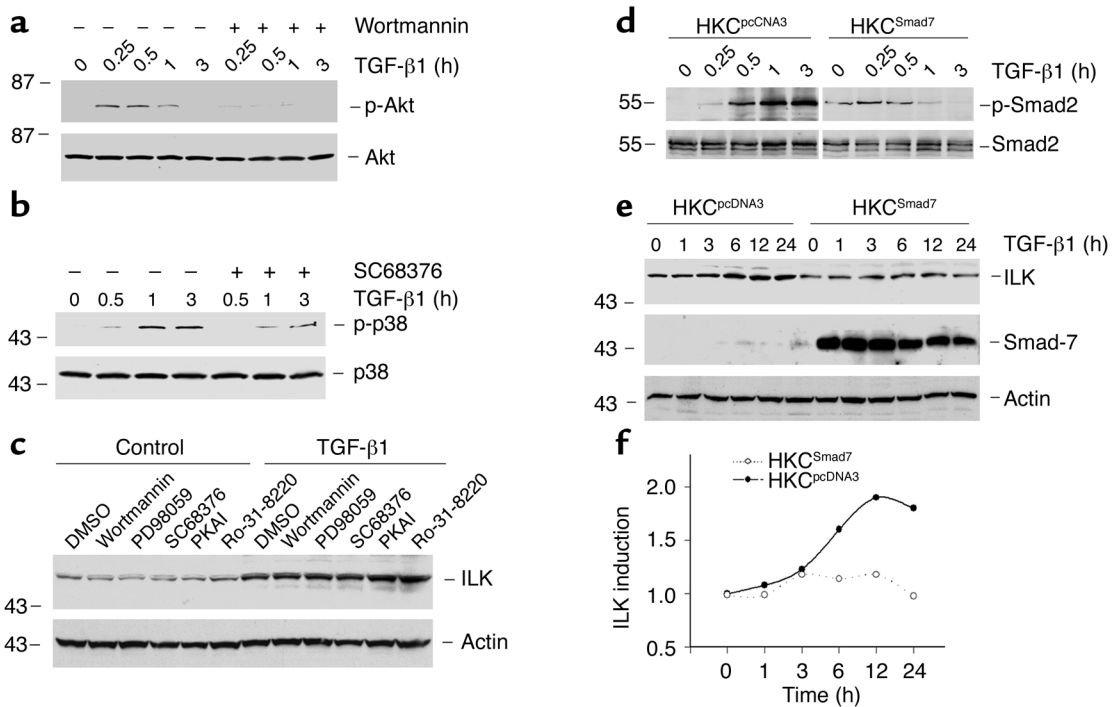


Figure 2

ILK induction by TGF- β 1 in renal epithelial cells is dependent on Smad signaling. (a-c) Pharmacological inhibition of different signal transduction pathways does not affect ILK induction by TGF- β 1. HKC cells were pretreated with either various chemical inhibitors or vehicle (DMSO) for 30 minutes, followed by incubating in the absence or presence of 2 ng/ml TGF- β 1 for 0.25, 0.5, 1 hour, 3 hours (a and b) and for 24 hours (c), respectively. Specific inhibitors for PI3K (10 nM wortmannin), Mek1 (10 μ M PD98059), p38 MAPK (20 μ M SC68376), PKA (0.3 μ M PKA inhibitor [PKAI]), and PKC (50 nM Ro-31-8220) were used, respectively. Cell lysates were immunoblotted with Ab's against phosphospecific Akt (p-Akt) and total Akt (a), phosphospecific and total p38 MAPK (p-p38 and p38, respectively) (b), ILK, and actin (c), respectively. (d-f) Overexpression of inhibitory Smad-7 abolishes ILK induction by TGF- β 1. A stable cell line overexpressing inhibitory Smad-7 (HKC^{Smad7}) was established by transfection of Smad-7 expression vector. A cell line with mock transfection of empty pcDNA3 vector (HKC^{pcDNA3}) was used as control. Cells were treated with 2 ng/ml of TGF- β 1 for various periods of time as indicated. (d) Cell lysates were blotted with phosphospecific (p-Smad2) and total Smad-2, respectively. (e) Cell lysates were blotted with Ab's against ILK, Smad-7, and actin, respectively. (f) Graphical presentation of relative ILK abundance normalized to actin following TGF- β 1 treatment in HKC^{pcDNA3} and HKC^{Smad7} cells. AU, arbitrary units.

ANOVA followed by the Student-Newman-Keuls test. A *P* value of less than 0.05 was considered significant.

Results

Induction of ILK during tubular EMT. Following incubation with TGF- β 1, renal tubular epithelial cells undergo EMT, a phenotypic conversion characterized by sequentially losing epithelial marker and acquiring characteristic features of mesenchyme (2). To investigate the potential involvement of ILK in this transition process, we examined the expression of ILK in renal tubular epithelial cells during EMT induced by TGF- β 1. As shown in Figure 1, treatment of HKC cells with TGF- β 1 at a concentration of 2 ng/ml induced ILK protein expression in a time-dependent manner. Western blot analyses revealed that endogenous ILK started to increase as early as 1 hour after treatment, and reached the peak at 48 hours after treatment. This induction of ILK by TGF- β 1 in renal tubular epithelial cells was also dose-dependent (Figure 1, b and d). Maximal induction of ILK was found at 5 ng/ml of TGF- β 1;

a further increase in TGF- β 1 concentration beyond this level did not cause further induction of ILK.

Immunofluorescence staining also illustrated an increase in cellular ILK in tubular epithelial cells after TGF- β 1 treatment (Figure 1, e and f). ILK was predominantly clustered in focal adhesions that have close contacts between the substrate and the plasma membrane on the basal surface of the cells (32) (Figure 1f). Despite dramatic induction, cellular localization of ILK exhibited a similar pattern after TGF- β 1 treatment (Figure 1f).

ILK induction by TGF- β 1 is dependent on intracellular Smad signaling. To unravel the mechanism by which TGF- β 1 induces ILK expression in tubular epithelial cells, we investigated the effects of blockade of various signaling pathways of TGF- β 1 on ILK expression. TGF- β 1 activated several distinctive signaling pathways in HKC cells, such as Smad-2 (Figure 2d), p38 MAPK (Figure 2b), and Akt (also known as protein kinase B) (Figure 2a). However, inhibition of p38 MAPK with specific chemical inhibitor SC68376 did not block ILK induction by TGF- β 1 (Figure 2c).

Similarly, blockage of Akt activation by wortmannin also failed to abolish TGF- β 1-initiated ILK expression. Likewise, neither Mek1 inhibitor PD98059 nor PKA and PKC inhibitors displayed any influence on ILK induction initiated by TGF- β 1 (Figure 2c).

To examine the potential involvement of Smad signaling in ILK induction, inhibited Smad signaling through overexpression of inhibitory Smad-7. Because Smad-7 competes with Smad-2 and Smad-3 to bind to activated TGF- β type I receptor, this presumably leads to attenuation of Smad signaling transduced by Smad-2/3. To this end, stably transfected cell line HKC^{Smad7} was established by transfecting HKC cells with Smad-7 expression vector, followed by selecting in medium containing G418. As shown in Figure 2e, Smad-7 overexpression was confirmed by Western blot analysis. In contrast to vector-transfected cells (HKC^{pcDNA3}), Smad-7 overexpression in HKC cells abolished TGF- β 1-induced Smad-2 phosphorylation (Figure 2d) and ILK expression (Figure 2, e and f). These results are consistent with the notion that ILK induction by TGF- β 1 is primarily mediated through Smad signaling in renal tubular epithelial cells.

Ectopic expression of ILK induces loss of epithelial marker E-cadherin. To investigate the cellular consequence of ILK induction by TGF- β 1 in tubular epithelial cells, we

studied the effects of ILK overexpression on renal epithelial cell phenotype by stable transfection of WT-ILK expression vector. Three individual cell lines (WT-ILK-C1, -C2, and -C3) with different levels of WT-ILK expression as well as a cell line with overexpression of a dominant-negative kd-ILK were established. In addition, a cell line with mock transfection of empty vector pUSEamp was established as a negative control.

Because E-cadherin is an epithelial marker that plays an essential role in the maintenance of epithelial integrity, and because its loss is the earliest key cellular event during tubular EMT induced by TGF- β 1 (2), we initially examined the effects of ILK overexpression on E-cadherin protein levels. As shown in Figure 3a, forced expression of WT-ILK markedly suppressed endogenous E-cadherin protein expression, as demonstrated by Western blot analysis. In contrast, ectopic expression of kd-ILK did not inhibit E-cadherin expression in tubular epithelial cells (Figure 3a). Of interest, there was a close inverse correlation between ILK levels and E-cadherin abundance, suggesting a dose-dependent effect of ILK on E-cadherin expression. For instance, in the cell line with the highest level of ILK expression, WT-ILK-C3, endogenous E-cadherin protein was virtually absent. Quantitative results by densitometric analysis of the Western blots

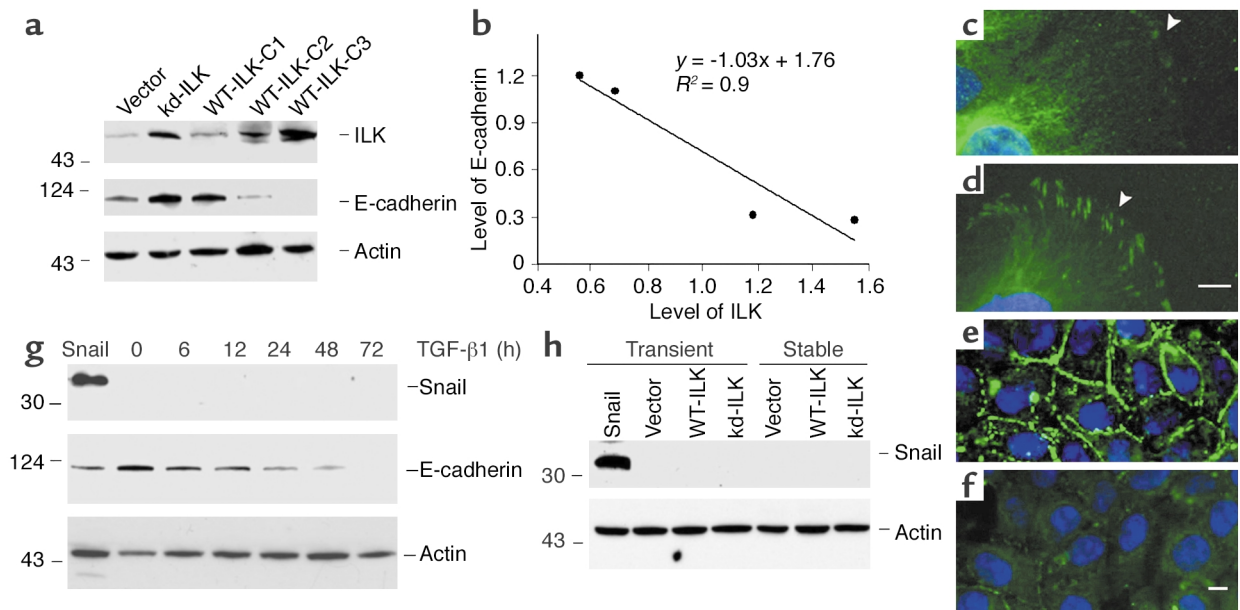


Figure 3

Forced expression of ILK suppresses E-cadherin expression in tubular epithelial cells in a dose-dependent manner. Stable cell lines were established by transfection of WT-ILK and kd-ILK expression vectors. A cell line with mock transfection of empty vector pUSEamp plasmid (Vector) was used as control. (a) Cell lysates were immunoblotted with Ab's against ILK, E-cadherin, and actin, respectively. Numbers (C1, C2, and C3) indicate three individual clones that express different levels of ILK. (b) Linear regression shows a close association between ILK and E-cadherin in tubular epithelial cells. The correlation coefficients (R^2) are shown. The relative abundances of ILK and E-cadherin were normalized to actin. (c-f) Immunofluorescence staining shows an inverse relationship between ILK and E-cadherin expression in HKC cells transfected with empty vector (c and e) or WT-ILK (d and f). (c and d) ILK staining. (e and f) E-cadherin staining. Scale bars, 5 μ m. (g and h) Suppression of E-cadherin expression by ILK is independent of Snail. Neither TGF- β 1 (g) nor ILK (h) induced Snail expression in tubular epithelial cells. HKC cells were treated with 2 ng/ml of TGF- β 1 for various periods of time as indicated (g), or transfected (either transiently or stably) with WT-ILK and kd-ILK expression vectors (h). HKC cells transiently transfected with Snail expression vector served as positive control for Snail protein expression.

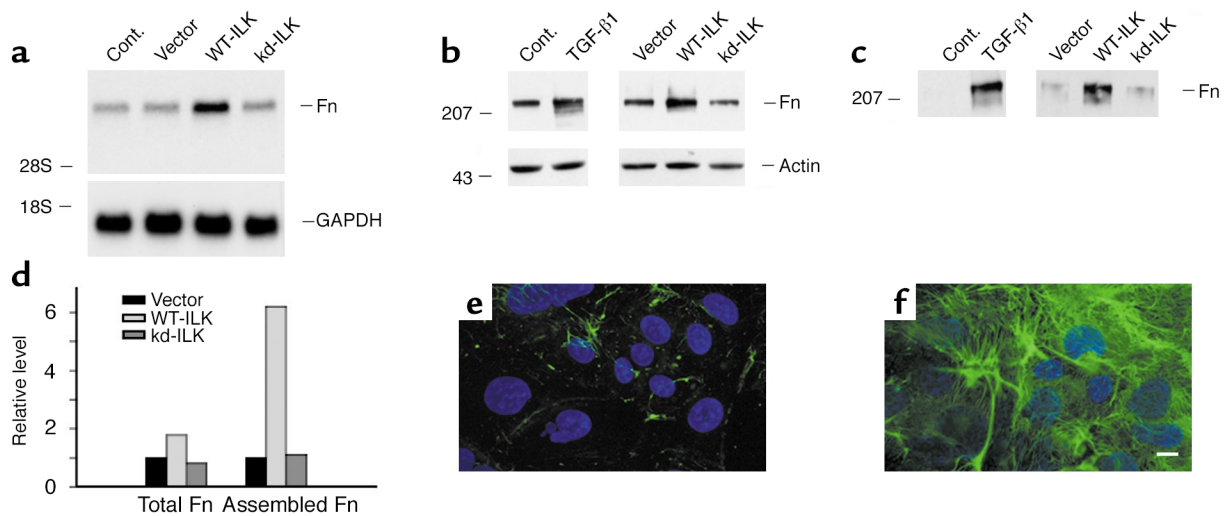


Figure 4

Forced expression of ILK induces fibronectin expression and its extracellular assembly. (a) Northern blot analysis shows that forced expression of ILK induces fibronectin (Fn) mRNA expression in tubular epithelial cells. Total RNA was isolated from different cell lines as indicated and hybridized with cDNA probes of fibronectin and GAPDH, respectively. Cont., control parental HKC cells; vector, HKC cells transfected with empty vector. (b) Western blot demonstrates that either treatment with TGF- β 1 or forced expression of ILK induced total fibronectin protein expression in tubular epithelial cells. Cell lysates were immunoblotted with Ab's against fibronectin and actin, respectively. (c) Expression of ILK promotes the extracellular assembly of fibronectin. Extracellular protein extracts were prepared from various cells as indicated and subjected to Western blot analyses using fibronectin Ab. (d) Graphical presentation shows the effects of ILK expression on the relative extent of total fibronectin expression and its extracellular assembly. Data are presented as fold induction over the empty vector control cells. (e and f) Immunofluorescence staining demonstrates the extracellular assembly of fibronectin in tubular epithelial cells transfected with empty vector (e) or WT-ILK (f). Scale bar, 5 μ m.

were plotted after normalization with actin. Figure 3b shows the regression line equation and correlation coefficients. Of note, because of its high level of ILK expression, we used mainly the WT-ILK-C3 cell line for subsequent experiments (see below).

The suppression of E-cadherin expression by ILK was further confirmed by immunofluorescence staining. Figure 3, c-f, shows the immunostaining results for ILK and E-cadherin in the WT-ILK-C3 cells and control cells, respectively. Strong staining for E-cadherin was visible in the plasma membrane of the control tubular epithelial cells (Figure 3e). However, E-cadherin staining largely disappeared in the WT-ILK-C3 cells (Figure 3f).

Because previous studies suggest a role of Snail transcription factor in E-cadherin repression in tumor epithelial cells, we further investigated the potential involvement of Snail in mediating TGF- β 1-triggered E-cadherin suppression in tubular epithelial cells. As shown in Figure 3g, there was no detectable Snail protein in HKC cells under basal conditions, and TGF- β 1 did not induce its expression at different timepoints tested. Despite the lack of Snail induction, TGF- β 1 suppressed E-cadherin expression in a time-dependent manner (Figure 3g). Transfection of Snail expression vector as a positive control resulted in marked Snail expression and moderate E-cadherin repression. Neither transient nor stable transfection of WT-ILK or kd-ILK induced Snail expression in HKC cells (Figure 3h).

These results suggest that ILK mediates TGF- β 1-triggered E-cadherin repression by a mechanism independent of Snail transcription factor in tubular epithelial cells.

Expression of ILK induces fibronectin expression and its extracellular assembly. One of the cellular consequences of EMT is production of massive interstitial matrix components. Along this line, we examined the effects of ILK on fibronectin expression in ILK-overexpressing tubular epithelial cells. As shown in Figure 4a, Northern blot analysis revealed that ectopic expression of WT-ILK induced fibronectin mRNA expression in HKC cells. Under the same conditions, no fibronectin mRNA induction was found in HKC cells transfected with either kd-ILK or empty vector (Figure 4a). Accordingly, the cellular level of fibronectin protein was also significantly increased in WT-ILK-overexpressing cells, but not in the cells expressing kd-ILK or empty vector (Figure 4b). Of note, the magnitude of fibronectin induction in WT-ILK-overexpressing cells was comparable to that stimulated by TGF- β 1. This suggests that TGF- β 1-initiated fibronectin induction is mainly mediated by the increased expression of ILK.

We also examined the extracellular assembly of fibronectin by a biochemical assay. The abundance of fibronectin in the ECM preparations from different cell lines was determined by Western blot analysis. As shown in Figure 4c, ectopic expression of WT-ILK dramatically increased fibronectin assembly in the

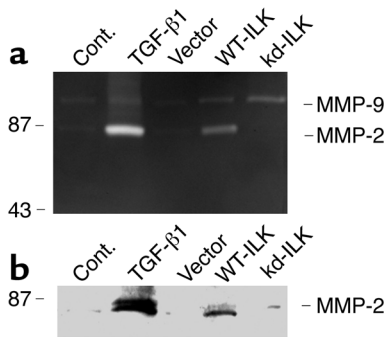


Figure 5 Expression of ILK induces MMP-2 expression and secretion by tubular epithelial cells. (a) Zymographic analysis shows the proteolytic activity of MMP-2 and MMP-9 in the supernatants of different cell lines. The locations of MMP-9 and MMP-2 are indicated. The samples from HKC cells treated without or with 2 ng/ml of TGF-β1 were loaded in the adjacent lanes to serve as controls for MMP-2 induction. (b) Western blot analysis demonstrates that expression of ILK induces MMP-2 expression by tubular epithelial cells. Equal amounts of the supernatants derived from the HKC lines with overexpression of either WT-ILK, kd-ILK, or empty vector were immunoblotted with specific Ab against MMP-2.

extracellular compartment. However, expression of kd-ILK in HKC cells failed to significantly influence fibronectin assembly. Consistently, the magnitude of the increase in assembled fibronectin in both WT-ILK-overexpressing cells and the HKC cells stimulated with TGF-β1 was similar, suggesting that ILK is as effective as TGF-β1 in promoting extracellular assembly of fibronectin. Quantitative determination revealed a more than sixfold induction of fibronectin assembly in the extracellular compartment in ILK-overexpressing cells compared with control cells (Figure 4d). This degree of induction in fibronectin assembly was clearly greater than that elicited by an increase in mRNA and total fibronectin protein, which was approximately twofold (Figure 4, a, b, and d). These results imply that ILK not only induces fibronectin expression, but perhaps more importantly, it preferentially promotes the extracellular assembly of fibronectin.

Figure 4, e and f, shows the localization of fibronectin in WT-ILK-C3 and control cells as illustrated by immunofluorescence staining. Fibronectin was present as assembled fibrils predominantly located at the extracellular compartment of the

cells. Consistently, ectopic expression of WT-ILK markedly induced fibronectin abundance and its extracellular assembly (Figure 4f).

Expression of ILK induces MMP-2 expression and promotes cell migration and invasion. We further investigated whether ILK mediates the induction of MMP-2 expression, a key event that plays a critical role in disrupting the tubular basement membrane (TBM) integrity of renal tubules (2, 4, 5). To this end, we examined MMP-2 expression by Western blot and zymographic analysis, respectively. As shown in Figure 5, MMP-2 protein was induced in ILK-overexpressing cells compared with that in the control or kd-ILK-expressing cells. However, the magnitude of this induction was smaller than that induced by TGF-β1, suggesting that additional pathways besides ILK may be implicated in MMP-2 induction by TGF-β1. Of interest, overexpression of both WT-ILK and kd-ILK slightly induced MMP-9 expression (Figure 5a).

Figure 6, a and b, shows the results of a cell motility assay using a Boyden chamber system. HKC cells overexpressing WT-ILK displayed a greater ability to migrate than controls. Quantitative determination demonstrated an increase of approximately fourfold in the number of cells migrating across the Transwell filters (Figure 6c). We also examined the effects of ILK overexpression on cell invasion capacity in three-dimensional Matrigels. As shown in Figure 6, d-f, when the WT-ILK-C3 cells were placed on top of Matrigel, they clearly invaded the Matrigel and migrated toward

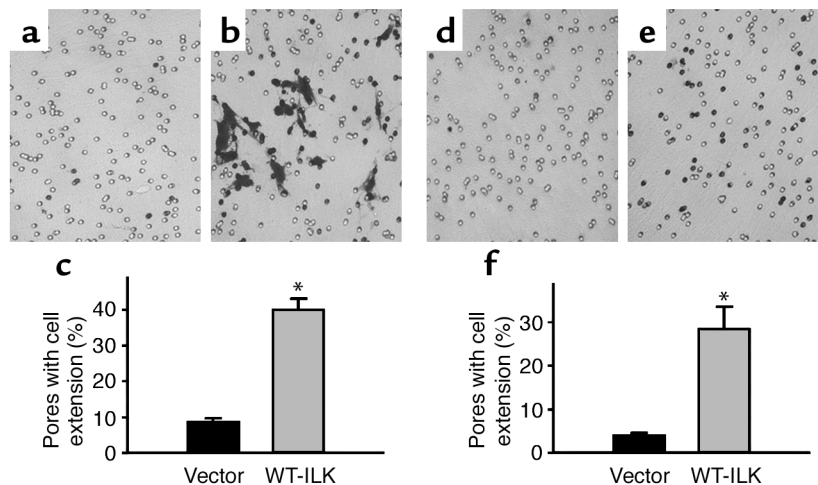


Figure 6 Forced expression of ILK enhances the migration and invasion capacity of tubular epithelial cells. (a-c) Boyden chamber motility assay demonstrates enhanced cell migration in tubular epithelial cells overexpressing ILK. Control (vector) (a) and ILK-overexpressing WT-ILK-C3 (b) cells were seeded on Transwell membranes and incubated for 5 days. Cells and cell extensions that migrated through the pores of Transwell plates were counted and reported (c). * $P < 0.01$, $n = 3$. (d-f) Matrigel invasion assay shows an enhanced invasion capacity of the tubular epithelial cells overexpressing ILK. Control (empty vector) (d) and ILK-overexpressing WT-ILK-C3 (e) cells were seeded on top of Matrigel in the Transwell filters of the Boyden chamber and incubated for 5 days. Cell extensions that invaded the Matrigel and migrated through the pores of the Transwell plates were counted and reported (f). * $P < 0.01$, $n = 3$.

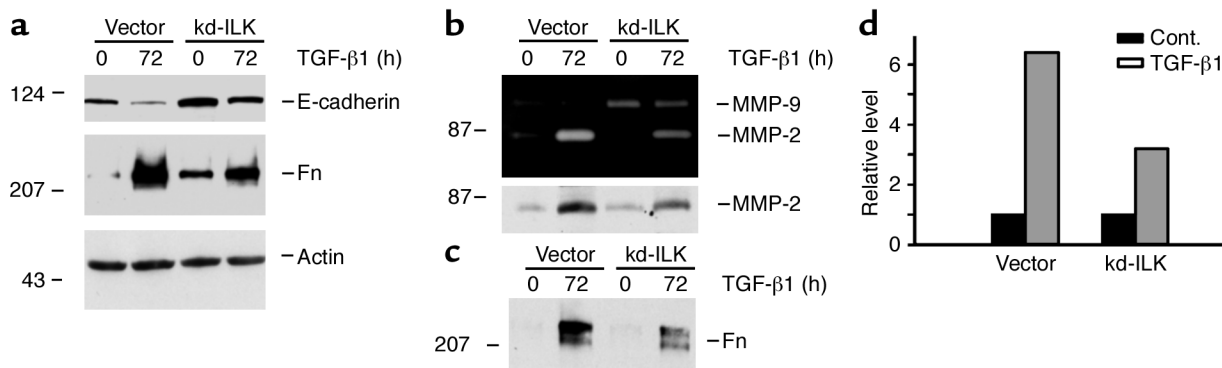


Figure 7

Ectopic expression of kd-ILK largely blocks TGF- β 1-induced phenotypic transition of tubular epithelial cells. (a) HKC cells transfected with empty vector or kd-ILK were incubated with or without 2 ng/ml of TGF- β 1 for 72 hours. Western blot analyses demonstrate that ectopic expression of kd-ILK largely blocked TGF- β 1-initiated E-cadherin suppression and fibronectin induction in tubular epithelial cells. (b) Zymographic analysis (upper panel) and Western blot (lower panel) show that expression of kd-ILK reduces MMP-2 expression induced by TGF- β 1. (c and d) Expression of kd-ILK attenuates the extracellular assembly of fibronectin after TGF- β 1 treatment. Extracellularly assembled fibronectin was analyzed by Western blot analyses (c). Graphical presentation (d) shows the effect of kd-ILK expression on the relative abundance of assembled fibronectin induced by TGF- β 1. Data are presented as fold induction over cells not treated with TGF- β 1.

the Transwell filters, so that the pores of the Transwell filters were filled with cell extensions. The number of WT-ILK-C3 cells that reached the basal surface of the Matrigel, as demonstrated by pores filled with cell extensions, was greater than the number of control cells that did the same (Figure 6f).

We also found that cells with ectopic expression of ILK displayed an altered morphology. HKC cells overexpressing ILK exhibited an elongated, spindle-like shape compared with control cells (data not shown). However, overexpression of ILK did not significantly affect cell proliferation. The growth rate of the WT-ILK-C3 cells was similar to that of the controls (data not shown).

Forced expression of kd-ILK blocks TGF- β 1-induced tubular EMT. To understand whether ILK induction is necessary for mediating TGF- β 1-induced tubular EMT, we investigated the effects of overexpressing a dominant-negative, kinase-dead form of ILK on mesenchymal conversion of tubular epithelial cells induced by TGF- β 1. This dominant-negative strategy presumably attenuates the action of elevated ILK induced by TGF- β 1. As described above, ectopic expression of kd-ILK did not significantly affect E-cadherin (Figure 3a) or fibronectin (Figure 4b) expression under basal conditions. However, expression of kd-ILK largely abolished TGF- β 1-induced E-cadherin suppression and fibronectin induction (Figure 7a), the hallmarks of tubular epithelial cell phenotypic conversion. Likewise, overexpression of kd-ILK also partially blocked MMP-2 expression induced by TGF- β 1 (Figure 7b), although kd-ILK slightly induced MMP-9 expression by HKC cells. As shown in Figure 7, c and d, ectopic expression of the dominant-negative kd-ILK also blocked TGF- β 1-induced fibronectin assembly in the extracellular compartment. Collectively, these results indicate

that ILK induction plays a critical role in mediating TGF- β 1-initiated tubular EMT.

Induction of ILK during tubular EMT in the fibrotic kidney. To provide evidence for a role of ILK in tubular EMT in vivo, we investigated the expression of ILK in the kidney in a model of renal interstitial fibrosis induced by UUU. As illustrated in Figure 8, a and b, ureteral obstruction markedly induced ILK expression in the kidney in a time-dependent fashion. A marked increase in ILK protein was evident in the obstructed kidneys as early as 1 day after surgery, and peaked at 7 days after surgery, a timepoint significantly preceding and/or coinciding with maximal tubular EMT in this model (2, 4). Northern blot analysis also revealed a time-dependent induction of ILK mRNA in the fibrotic kidneys (data not shown).

Immunofluorescence staining showed that the induction of ILK was largely limited to tubular epithelium, but not in the interstitial compartment (Figure 8, f-k). Double staining for ILK (red) and tubular marker (green) demonstrated that strong staining for ILK protein was specifically localized in renal tubules of obstructed kidneys, whereas ILK staining was virtually absent in sham control kidneys. Of interest, at 3 days after UUU, ILK staining was predominantly localized along the basal region of renal tubules, presumably the contact sites between the TBM and the plasma membrane of the tubular epithelial cells (Figure 8, f-h). However, ILK was present in the entire tubules of the diseased kidneys at 7 days after UUU (Figure 8, i-k), suggesting a shift of ILK localization in the process of renal fibrogenesis. Hence, there is close temporal and spatial correlation between ILK induction and tubular EMT in this model.

We also examined ILK expression in the kidney in diabetic nephropathy. A uninephrectomized diabetic model was used because earlier studies show that

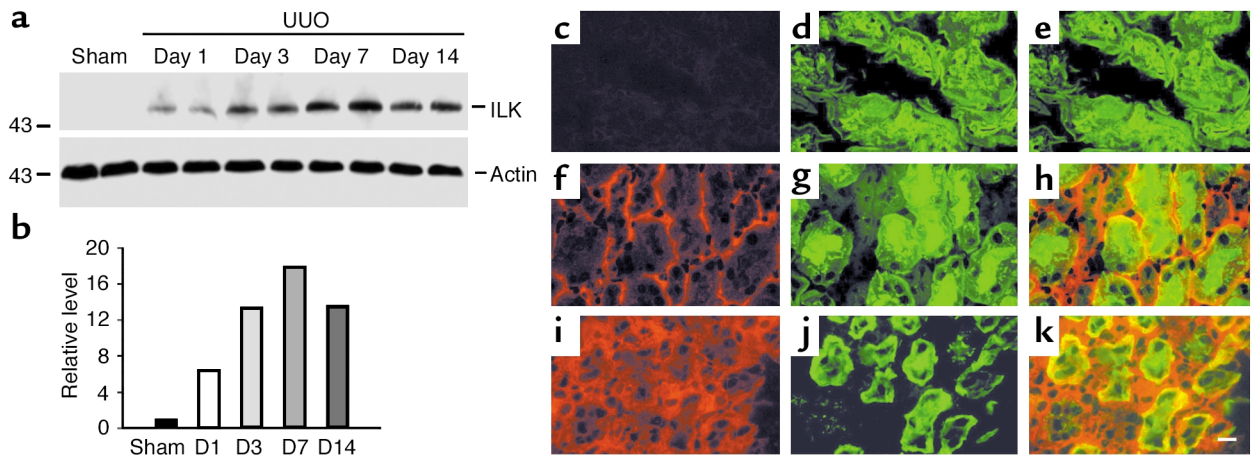


Figure 8

Induction of ILK expression occurs specifically in renal epithelia in obstructive nephropathy. (a and b) Western blot analysis shows marked induction of ILK in the fibrotic kidney induced by UUO in a time-dependent manner. Kidney homogenates were immunoblotted with Ab's against ILK and actin, respectively. The relative abundances of ILK are presented in b after normalization with actin. Samples from two individual animals were used at each timepoint. (c-k) Immunofluorescence staining shows localization of ILK (red) and the tubular cell marker lectin (green) in the sham kidney (c-e) and obstructed kidneys after 3 (f-h) and 7 days (i-k), respectively. Scale bar, 20 μ m.

uninephrectomy markedly accelerates the progression of renal fibrotic lesions in diabetic animals (30). Compared with normal control, uninephrectomized diabetic mice at 3 months after injection of streptozotocin developed severe diabetic nephropathy. Urine albumin ($1,479.7 \pm 594.4$ vs. 23.4 ± 8.6 μ g/mg creatinine; diabetic vs. normal; $P < 0.01$), serum creatinine (0.22 ± 0.02 vs. 0.17 ± 0.02 mg/dl; diabetic vs. normal; $P < 0.05$), and urine TGF- β 1 level (25.2 ± 3.8 vs. 1.0 ± 0.3 ng/mg creati-

nine; diabetic vs. normal; $P < 0.01$) were markedly increased in uninephrectomized diabetic mice. Significant glomerular injuries including mesangial expansion, matrix deposition, and cell apoptosis as well as interstitial fibrotic lesions were evident in uninephrectomized diabetic mice at this stage (data not shown).

Figure 9a shows an increase in ILK expression in diabetic kidneys at 3 months after injection of streptozotocin, compared with normal control. Immunofluo-

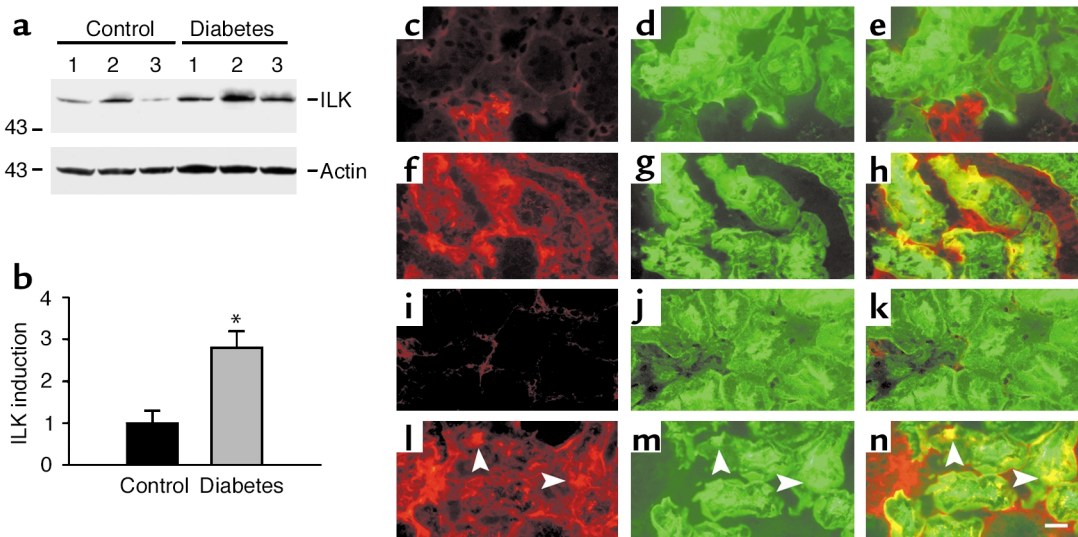


Figure 9

Induction of ILK expression in renal epithelia in diabetic nephropathy is associated with tubular EMT. (a and b) Western blot analysis shows induction of ILK expression in diabetic nephropathy in mice. Whole-tissue homogenates derived from control or diabetic mice were immunoblotted with Ab's against ILK and actin, respectively. The relative abundance of ILK (fold induction) is presented in b after normalization with actin. $*P < 0.05$ ($n = 3$). (c-h) Immunofluorescence staining shows localization of ILK (red) and the tubular cell marker lectin (green) in control (c-e) and diabetic kidneys (f-h), respectively. (i-n) Immunofluorescence staining demonstrates tubular EMT in diabetic nephropathy, as illustrated by colocalization of α -smooth muscle actin (red) and lectin (green) in diabetic kidneys (l-n) (arrowheads). (i-k) Control kidney. Scale bar, 20 μ m.

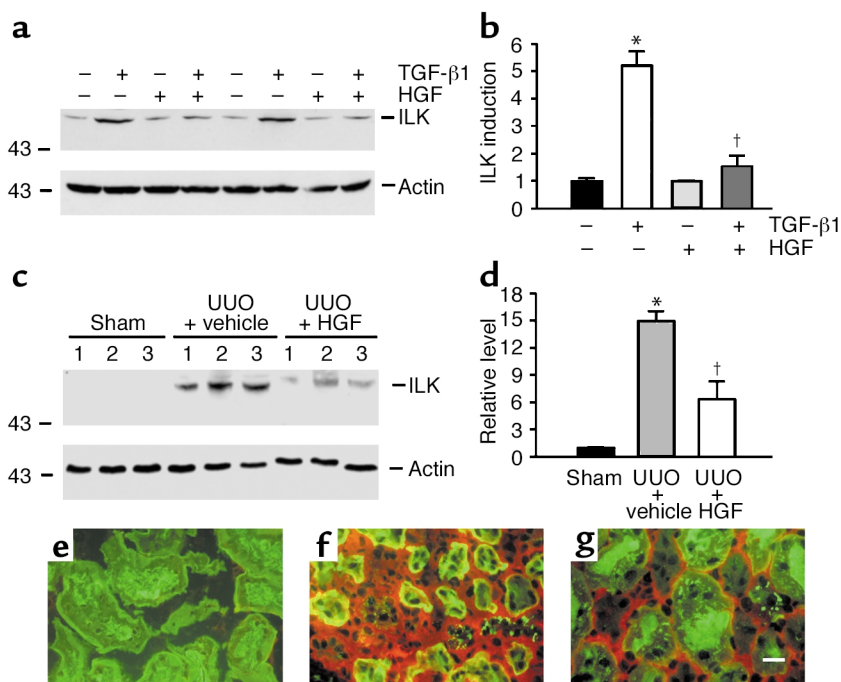


Figure 10 Inhibition of ILK expression in tubular epithelial cells by HGF in vitro and in vivo. (a and b) HGF inhibits ILK expression induced by TGF- β 1 in tubular epithelial cells in vitro. HKC cells were treated with TGF- β 1 (2 ng/ml), HGF (40 ng/ml), or both for 48 hours. Representative Western blot (a) and graphical presentation (b) show the relative abundances of ILK (fold induction) after various treatments. Data are presented as mean \pm SEM of three independent experiments. * $P < 0.01$ vs. normal control; † $P < 0.01$ vs. TGF- β 1 alone. (c and d) HGF inhibits renal ILK expression in obstructive nephropathy. Whole-tissue homogenates derived from the kidneys at 7 days after surgery were immunoblotted with Ab's against ILK and actin, respectively. The relative abundances of ILK (fold induction) are presented in d after normalization with actin. * $P < 0.01$ vs. sham; † $P < 0.01$ vs. vehicle control ($n = 3$). (e-g) Double immunofluorescence staining shows localization of ILK (red) and the tubular cell marker lectin (green) in the kidneys at 7 days after surgery in the sham (e), UUO with vehicle (f), and UUO with HGF (g) groups, respectively. Scale bar, 20 μ m. Inhibition of ILK expression by HGF is accompanied by blockage of tubular EMT and attenuation of renal fibrosis, as previously reported (6).

rescence staining revealed that the induction of ILK expression was largely confined to the renal tubular compartment (Figure 9, c-h). Unlike the glomeruli that displayed weak staining for ILK in basal conditions, proximal tubular epithelial cells were essentially negative for ILK in normal kidney (Figure 9, c-e), suggesting de novo ILK expression in tubular epithelia under diabetic conditions. Of interest, this tubular ILK expression was accompanied by a phenotypic conversion of tubular epithelial cells, as illustrated by colocalization of tubular marker and α -smooth muscle actin (Figure 9, i-n). Taken together, these results indicate that ILK is also induced in the tubular epithelia in diabetic kidney, and that such ILK induction is associated with tubular EMT.

Inhibition of ILK expression by HGF blocks TGF- β 1-initiated EMT and attenuates renal fibrosis. Previous studies from our laboratory demonstrated that HGF specifically blocks tubular EMT and attenuates renal fibrosis both in vitro and in vivo (6). Given a critical role of ILK in mediating EMT as described

above, we reasoned that HGF may exert its action by inhibiting ILK expression. As shown in Figure 10, a and b, simultaneous incubation of HKC cells with HGF almost completely abolished ILK induction triggered by TGF- β 1. Of note, HGF did not affect basal ILK expression in HKC cells. Inhibition of ILK expression by HGF was accompanied by blockage of TGF- β 1-initiated tubular EMT, as demonstrated by HGF preservation of E-cadherin expression and inhibition of fibronectin expression (data not shown), as described previously (6).

As shown in Figure 10, c and d, HGF inhibited ILK expression in the fibrotic kidney induced by UUO. Intravenous administration of HGF largely abrogated ILK induction in the obstructed kidney at 7 days after ureteral ligation. This inhibition of ILK expression by HGF was independently confirmed by immunofluorescence staining (Figure 10, e-g). Of note, inhibition of ILK expression by HGF in vivo was associated with blockade of tubular EMT and attenuation of renal fibrosis in this model (data not shown) (6).

Discussion

The results presented in this paper implicate ILK as a crucial mediator of mesenchymal transformation from tubular epithelial cells in the pathogenesis of renal interstitial fibrosis. This conclusion is supported by several lines of observation. First, endogenous ILK expression in tubular epithelial cells is induced by TGF- β 1, a profibrotic cytokine that has been shown to initiate tubular EMT in vitro (2, 8). Second, forced expression of exogenous ILK induces numerous key events including loss of the epithelial cell-cell adhesion molecule E-cadherin, induction of fibronectin expression and its extracellular assembly, induced MMP-2 expression and secretion, and enhanced cell migration and invasion. This virtually recapitulates the major events during the entire course of tubular EMT induced by TGF- β 1 (2), underscoring that ILK is perhaps sufficient for mediating tubular EMT. Third, ectopic expression of a dominant-negative, kinase-dead form of ILK largely

abrogates TGF- β 1-initiated E-cadherin suppression and fibronectin induction and assembly (Figure 8), corroborating the notion that ILK signaling is necessary for mediating TGF- β 1's action in tubular EMT. Fourth, ILK induction is specifically confined to renal tubular epithelium and coincides with tubular EMT in two models of chronic renal fibrosis induced by either obstructive insult or diabetic injury in mice, indicating a spatial and temporal association between ILK and tubular EMT *in vivo*. Finally, inhibition of ILK induction by HGF blocks TGF- β 1-initiated tubular EMT *in vitro* and attenuates renal interstitial fibrosis *in vivo*. Collectively, these results present convincing arguments supporting a critical role for ILK in mediating tubular EMT. Our findings shed new light on identifying the molecular mediator and elucidating the mechanism underlying tubular EMT in the pathogenesis of chronic renal fibrosis.

Previous studies have demonstrated that tubular EMT is an orchestrated process that is regulated by a coordinated alteration in gene expression (2, 12). It is conceivable that the completion of the tubular EMT process depends on proper interaction of tubular cells with ECM via integrin-mediated signaling. In light of its central position in the crossroads connecting the integrins and the actin cytoskeleton (17, 18), ILK was hypothesized to be a candidate signaling molecule that plays a role in mediating TGF- β 1-initiated tubular EMT. In this study, we have clearly demonstrated that ILK is a downstream effector of TGF- β 1, because ILK is both sufficient and necessary for mediating tubular EMT (Figure 3 through Figure 7), and because its expression in tubular epithelial cells is tightly controlled by TGF- β 1 (Figure 1). In accordance with this, it has been demonstrated that TGF- β 1 induces ILK expression in human HT-144 melanoma cell lines (33). Of interest, despite the fact that TGF- β 1 is capable of activating several signal transduction pathways (27, 34, 35), ILK induction by TGF- β 1 is clearly dependent upon intact Smad signaling in tubular epithelial cells, since overexpression of inhibitory Smad-7 abolishes Smad-2 phosphorylation and ILK induction (Figure 2). Consistently, overexpression of Smad-7 also blocks tubular EMT induced by TGF- β 1 (36). Of note, although RhoA has been implicated in EMT (37, 38), TGF- β 1-induced RhoA activation in tubular epithelial cells is neither dependent on Smad signaling nor on ILK (Y. Li et al., unpublished data). This suggests that Smad/ILK and RhoA are two parallel signaling pathways initiated by TGF- β 1. Given the fact that RhoA is important only in TGF- β -induced stress fiber formation but not in the disruption of adherens and tight junctions (38), it is reasonable to assume that ILK acts as a major intermediate signaling molecule that couples TGF- β 1/Smad signaling and tubular EMT.

Through its interactions using distinct domains, ILK strategically bridges the integrins and actin cytoskeleton-associated proteins including PINCH, CH-ILKBP, and paxillin and transmits signal

exchanges between the intracellular and extracellular compartments (17, 39–41). In addition, ILK also couples integrins and growth factor receptors to downstream signaling components (17, 18). Among the many functions of ILK in diverse cellular processes, perhaps the chief one is to modulate cell adhesions (20, 42). Accordingly, a hallmark of ILK overexpression in epithelial cells is the loss of epithelial cell-cell adhesion by downregulation of E-cadherin expression (Figure 3) (20, 42). This is in agreement with our previous observation that suppression of E-cadherin expression is a key step that precedes other major events during tubular EMT induced by TGF- β 1 (2). Therefore, ectopic expression of ILK in tubular epithelial cells underlines that ILK signaling *per se* is sufficient for mediating TGF- β 1's action to initiate mesenchymal transformation of tubular epithelial cells. Because E-cadherin is an epithelial adhesion receptor that plays a pivotal role in the maintenance of the structural and functional integrity of tubular epithelium (43–45), downregulation of E-cadherin will presumably lead to destabilization of epithelial sheet integrity, making cells ready to lose polarity, to dissociate from their neighbors, and to migrate. Of note, downregulation of E-cadherin in renal tubular epithelium in obstructed kidney *in vivo* dominates at 7 days after UUO (2), a timepoint that is significantly preceded by induction of ILK (Figure 9). This implies that ILK could also be responsible for the disappearance of E-cadherin in renal tubules in fibrotic kidneys *in vivo*. The mechanism underlying E-cadherin suppression by ILK remains elusive. It has been previously shown that Snail transcription factor plays a critical role in suppressing E-cadherin expression in tumor epithelial cells (24, 46), and that ILK signaling is implicated in Snail expression (47). However, no detectable Snail protein was observed in HKC cells under basal conditions after stimulation with TGF- β 1 or following overexpression of ILK (Figure 3), suggesting that Snail expression is cell content-dependent. Hence, it is clear that ILK mediates TGF- β 1-triggered E-cadherin repression by a mechanism independent of Snail in tubular epithelial cells.

Another hallmark for tubular EMT is cells beginning to overproduce ECM components and to properly assemble in the extracellular compartment, leading to excess accumulation of ECM, causing massive tissue fibrosis as seen in diseased kidney. The present study has underscored that ILK is essential in both fibronectin gene expression and its deposition into ECM (Figure 4). The fact that both mRNA and cellular protein levels of fibronectin are increased in ILK-overexpressing cells indicates that ILK signaling is capable of influencing fibronectin gene expression. Nevertheless, judging from the magnitude of the induction of fibronectin extracellular assembly versus fibronectin expression (Figure 4), it is easy to recognize that ILK preferentially promotes fibronectin assembly. ILK localizes to both focal adhe-

sions and fibrillar adhesions (so-called ECM contacts) (16, 22), consistent with a role for ILK in fibronectin matrix assembly. Because these contacts are active sites for the deposition of fibronectin into ECM (48–51), this pattern of ILK localization underscores a direct role in promoting fibronectin assembly. Given a role for ILK in connecting integrins and actin cytoskeleton, it is likely that ILK promotes the deposition of fibronectin into ECM by influencing the activation of integrins and/or by providing a molecular scaffold for the assembly of integrins that mediate fibronectin assembly and the actin cytoskeleton-associated proteins (39). Regardless of the mechanism involved, our results establish that ILK is one crucial element in the cellular control of the deposition of fibronectin into ECM.

To complete tubular EMT *in vivo*, the transformed cells have to migrate into the interstitial compartment of the kidney. This task apparently requires coordinated actions to disrupt the TBM that normally confines tubular epithelial cells, and to allow the transformed cells to finally enter the interstitium. In this regard, it is of interest to point out that ILK is also involved in the regulation of cell migration, cell motility, and invasion in three-dimensional matrix. The observation that forced expression of ILK induces MMP-2 expression in tubular epithelial cells not only highlights that ILK can mimic TGF- β 1's action (2), but also suggests that MMP-2 may be responsible for TBM degradation and for the invasive phenotype of the transformed cells. Consistently, recent studies also indicate that ILK induces an invasive phenotype in brain tumor cell lines via AP-1-dependent upregulation of MMP-9 expression (52). In addition, its ability to phosphorylate myosin light chain may also hint at an important role for ILK in regulating cell motility (53). Accordingly, ILK induction in renal tubules is specifically localized at the basal region close to TBM in the early stage of obstructive injury (Figure 9), suggesting a crucial role of ILK in TBM degradation in the fibrotic kidney *in vivo*.

In view of an important role of ILK in mediating tubular EMT as described above, it is not difficult to envision a central role for ILK in the pathogenesis of renal fibrosis. Consistent with this view, emerging evidence suggests that dysregulation of ILK is implicated in various chronic glomerular diseases. For instance, ILK induction is found in glomerular podocytes, which is associated with progressive podocyte failure leading to proteinuria in animal models and in patients (21). It is also shown that increased ILK expression in mesangial cells is associated with diabetic glomerulosclerosis (22). The results in this study expand the correlation between ILK dysregulation and chronic renal fibrosis beyond the glomeruli. We have shown a tubule-specific induction of ILK in mouse kidney after both obstructive and diabetic injury, and such tubular ILK induction is closely associated with EMT and interstitial fibrosis

in these models (2, 3, 54). Of note, a dramatic induction of ILK (about 18-fold) in obstructive nephropathy (Figure 8) is consistent with a high incidence of EMT in this aggressive form of renal fibrosis (2, 3). In diabetic nephropathy, a moderate induction of ILK (about threefold) is associated with the low prevalence of EMT in the early phase of tubulointerstitial lesions in this model (54). Therefore, the frequency of tubular EMT in diseased kidneys is proportional to, and perhaps dictated by, the magnitude of ILK induction in renal epithelial cells after injury. In agreement with this notion, inhibition of ILK expression by HGF dramatically blocks tubular EMT and ameliorates renal fibrosis in obstructive nephropathy (Figure 10) (6). Hence, we propose a causative relationship between ILK upregulation and the activation of matrix-producing fibroblasts via EMT in renal fibrosis. More importantly, our study suggests a linear pathway that couples TGF- β 1, Smad signaling, ILK, tubular EMT, and renal interstitial fibrogenesis.

Given the facts that a dominant-negative, kinase-dead form of ILK largely abolishes TGF- β 1-induced tubular EMT and that inhibition of ILK expression by HGF blocks tubular EMT and reduces renal fibrosis, ILK signaling could be exploited as a novel therapeutic target for designing new treatment regimens for patients with chronic renal insufficiency. It is tempting to speculate that new strategies aimed at ILK expression and signaling may be effective at intercepting the profibrotic actions of TGF- β 1 and thereby halting the onset and progression of chronic renal fibrosis. Therefore, further studies are warranted to develop molecular tools that downregulate ILK expression (such as HGF) or disrupt ILK function (55), which allows us to intervene in ILK signaling for blockade of tubular EMT and for ultimate amelioration of the progressive loss of renal function in the fibrotic kidney.

Acknowledgments

We thank P. ten Dijke and A. Garcia de Herreros for generously providing plasmid vectors. This work was supported by NIH grants DK-54944, DK-61408, and DK-64005 to Y. Liu, and GM-65188 and DK-54639 to C. Wu. J. Yang and C. Dai were supported by postdoctoral fellowships from the American Heart Association Pennsylvania-Delaware Affiliate.

1. Strutz, F., and Muller, G.A. 2000. Transdifferentiation comes of age. *Nephrol. Dial. Transplant.* **15**:1729–1731.
2. Yang, J., and Liu, Y. 2001. Dissection of key events in tubular epithelial to myofibroblast transition and its implications in renal interstitial fibrosis. *Am. J. Pathol.* **159**:1465–1475.
3. Iwano, M., et al. 2002. Evidence that fibroblasts derive from epithelium during tissue fibrosis. *J. Clin. Invest.* **110**:341–350. doi:10.1172/JCI200215518.
4. Yang, J., et al. 2002. Disruption of tissue-type plasminogen activator gene in mice reduces renal interstitial fibrosis in obstructive nephropathy. *J. Clin. Invest.* **110**:1525–1538. doi:10.1172/JCI200216219.
5. Zeisberg, M., et al. 2001. Renal fibrosis: collagen composition and assembly regulates epithelial-mesenchymal transdifferentiation. *Am. J. Pathol.* **159**:1313–1321.
6. Yang, J., and Liu, Y. 2002. Blockage of tubular epithelial to myofibroblast transition by hepatocyte growth factor prevents renal interstitial fibrosis. *J. Am. Soc. Nephrol.* **13**:96–107.

7. Okada, H., Danoff, T.M., Kalluri, R., and Neilson, E.G. 1997. Early role of Fsp1 in epithelial-mesenchymal transformation. *Am. J. Physiol.* **273**:F563–F574.
8. Fan, J.M., et al. 1999. Transforming growth factor-beta regulates tubular epithelial-myofibroblast transdifferentiation in vitro. *Kidney Int.* **56**:1455–1467.
9. Strutz, F., et al. 2002. Role of basic fibroblast growth factor-2 in epithelial-mesenchymal transformation. *Kidney Int.* **61**:1714–1728.
10. Yang, J., Dai, C., and Liu, Y. 2002. Hepatocyte growth factor gene therapy and angiotensin II blockade synergistically attenuate renal interstitial fibrosis in mice. *J. Am. Soc. Nephrol.* **13**:2464–2477.
11. Border, W.A., and Noble, N.A. 1997. TGF-beta in kidney fibrosis: a target for gene therapy. *Kidney Int.* **51**:1388–1396.
12. Bottinger, E.P., and Bitzer, M. 2002. TGF-β1 signaling in renal disease. *J. Am. Soc. Nephrol.* **13**:2600–2610.
13. Schnaper, H.W., Hayashida, T., Hubchak, S.C., and Poncellet, A.C. 2003. TGF-beta signal transduction and mesangial cell fibrogenesis. *Am. J. Physiol. Renal Physiol.* **284**:F243–F252.
14. Eddy, A.A. 2000. Molecular basis of renal fibrosis. *Pediatr. Nephrol.* **15**:290–301.
15. Sutaria, P.M., Ohebsalom, M., McCaffrey, T.A., Vaughan, E.D., Jr., and Felsen, D. 1998. Transforming growth factor-beta receptor types I and II are expressed in renal tubules and are increased after chronic unilateral ureteral obstruction. *Life Sci.* **62**:1965–1972.
16. Wu, C. 2001. ILK interactions. *J. Cell Sci.* **114**:2549–2550.
17. Wu, C., and Dedhar, S. 2001. Integrin-linked kinase (ILK) and its interactors: a new paradigm for the coupling of extracellular matrix to actin cytoskeleton and signaling complexes. *J. Cell Biol.* **155**:505–510.
18. Dedhar, S., Williams, B., and Hannigan, G. 1999. Integrin-linked kinase (ILK): a regulator of integrin and growth-factor signalling. *Trends Cell Biol.* **9**:319–323.
19. Dedhar, S. 2000. Cell-substrate interactions and signaling through ILK. *Curr. Opin. Cell Biol.* **12**:250–256.
20. Wu, C., et al. 1998. Integrin-linked protein kinase regulates fibronectin matrix assembly, E-cadherin expression, and tumorigenicity. *J. Biol. Chem.* **273**:528–536.
21. Kretzler, M., et al. 2001. Integrin-linked kinase as a candidate downstream effector in proteinuria. *FASEB J.* **15**:1843–1845.
22. Guo, L., Sanders, P.W., Woods, A., and Wu, C. 2001. The distribution and regulation of integrin-linked kinase in normal and diabetic kidneys. *Am. J. Pathol.* **159**:1735–1742.
23. Nakao, A., et al. 1997. Identification of Smad7, a TGFbeta-inducible antagonist of TGF-beta signalling. *Nature.* **389**:631–635.
24. Battle, E., et al. 2000. The transcription factor snail is a repressor of E-cadherin gene expression in epithelial tumour cells. *Nat. Cell Biol.* **2**:84–89.
25. Racusen, L.C., et al. 1997. Cell lines with extended in vitro growth potential from human renal proximal tubule: characterization, response to inducers, and comparison with established cell lines. *J. Lab. Clin. Med.* **129**:318–329.
26. Liu, Y. 1999. Hepatocyte growth factor promotes renal epithelial cell survival by dual mechanisms. *Am. J. Physiol.* **277**:F624–F633.
27. Dai, C., Yang, J., and Liu, Y. 2003. Transforming growth factor-β1 potentiates renal tubular epithelial cell death by a mechanism independent of Smad signaling. *J. Biol. Chem.* **278**:12537–12545.
28. Oda, T., et al. 2001. PAI-1 deficiency attenuates the fibrogenic response to ureteral obstruction. *Kidney Int.* **60**:587–596.
29. Klahr, S., and Morrissey, J. 2002. Obstructive nephropathy and renal fibrosis. *Am. J. Physiol. Renal Physiol.* **283**:F861–F875.
30. Sato, Y., et al. 1995. Renoprotective effect of enalapril in uninephrectomized spontaneously hypertensive rats with neonatal streptozotocin-induced diabetes. *Diabetes Res. Clin. Pract.* **29**:153–161.
31. Liu, Y., et al. 1999. Up-regulation of hepatocyte growth factor receptor: an amplification and targeting mechanism for hepatocyte growth factor action in acute renal failure. *Kidney Int.* **55**:442–453.
32. Jockusch, B.M., et al. 1995. The molecular architecture of focal adhesions. *Annu. Rev. Cell Dev. Biol.* **11**:379–416.
33. Janji, B., Melchior, C., Vallar, L., and Kieffer, N. 2000. Cloning of an isoform of integrin-linked kinase (ILK) that is upregulated in HT-144 melanoma cells following TGF-beta1 stimulation. *Oncogene.* **19**:3069–3077.
34. Dennler, S., Goumans, M.J., and ten Dijke, P. 2002. Transforming growth factor beta signal transduction. *J. Leukoc. Biol.* **71**:731–740.
35. Massague, J. 2000. How cells read TGF-beta signals. *Nat. Rev. Mol. Cell Biol.* **1**:169–178.
36. Li, J.H., et al. 2002. Smad7 inhibits fibrotic effect of TGF-beta on renal tubular epithelial cells by blocking smad2 activation. *J. Am. Soc. Nephrol.* **13**:1464–1472.
37. Bhowmick, N.A., et al. 2001. Transforming growth factor-beta1 mediates epithelial to mesenchymal transdifferentiation through a RhoA-dependent mechanism. *Mol. Biol. Cell.* **12**:27–36.
38. Kaartinen, V., Haataja, L., Nagy, A., Heisterkamp, N., and Groffen, J. 2002. TGFbeta3-induced activation of RhoA/Rho-kinase pathway is necessary but not sufficient for epithelial-mesenchymal transdifferentiation: implications for palatogenesis. *Int. J. Mol. Med.* **9**:563–570.
39. Guo, L., and Wu, C. 2002. Regulation of fibronectin matrix deposition and cell proliferation by the PINCH-ILK-CH-ILKBP complex. *FASEB J.* **16**:1298–1300.
40. Tu, Y., Huang, Y., Zhang, Y., Hua, Y., and Wu, C. 2001. A new focal adhesion protein that interacts with integrin-linked kinase and regulates cell adhesion and spreading. *J. Cell Biol.* **153**:585–598.
41. Nikolopoulos, S.N., and Turner, C.E. 2002. Molecular dissection of actopaxin-integrin-linked kinase-Paxillin interactions and their role in subcellular localization. *J. Biol. Chem.* **277**:1568–1575.
42. White, D.E., Cardiff, R.D., Dedhar, S., and Muller, W.J. 2001. Mammary epithelial-specific expression of the integrin-linked kinase (ILK) results in the induction of mammary gland hyperplasias and tumors in transgenic mice. *Oncogene.* **20**:7064–7072.
43. Horster, M.F., Braun, G.S., and Huber, S.M. 1999. Embryonic renal epithelia: induction, nephrogenesis, and cell differentiation. *Physiol. Rev.* **79**:1157–1191.
44. Steinberg, M.S., and McNutt, P.M. 1999. Cadherins and their connections: adhesion junctions have broader functions. *Curr. Opin. Cell Biol.* **11**:554–560.
45. Knust, E., and Bossinger, O. 2002. Composition and formation of intercellular junctions in epithelial cells. *Science.* **298**:1955–1959.
46. Cano, A., et al. 2000. The transcription factor snail controls epithelial-mesenchymal transitions by repressing E-cadherin expression. *Nat. Cell Biol.* **2**:76–83.
47. Tan, C., et al. 2001. Inhibition of integrin linked kinase (ILK) suppresses beta-catenin-Lef/Tcf-dependent transcription and expression of the E-cadherin repressor, snail, in APC-/- human colon carcinoma cells. *Oncogene.* **20**:133–140.
48. Christopher, R.A., Kowalczyk, A.P., and McKeown-Longo, P.J. 1997. Localization of fibronectin matrix assembly sites on fibroblasts and endothelial cells. *J. Cell Sci.* **110**:569–581.
49. Pankov, R., et al. 2000. Integrin dynamics and matrix assembly: tensin-dependent translocation of alpha(5)beta(1) integrins promotes early fibronectin fibrillogenesis. *J. Cell Biol.* **148**:1075–1090.
50. Pankov, R., and Yamada, K.M. 2002. Fibronectin at a glance. *J. Cell Sci.* **115**:3861–3863.
51. Wu, C., Keivens, V.M., O'Toole, T.E., McDonald, J.A., and Ginsberg, M.H. 1995. Integrin activation and cytoskeletal interaction are essential for the assembly of a fibronectin matrix. *Cell.* **83**:715–724.
52. Troussard, A.A., et al. 2000. The integrin linked kinase (ILK) induces an invasive phenotype via AP-1 transcription factor-dependent upregulation of matrix metalloproteinase 9 (MMP-9). *Oncogene.* **19**:5444–5452.
53. Deng, J.T., Van Lierop, J.E., Sutherland, C., and Walsh, M.P. 2001. Ca2+-independent smooth muscle contraction. A novel function for integrin-linked kinase. *J. Biol. Chem.* **276**:16365–16373.
54. Oldfield, M.D., et al. 2001. Advanced glycation end products cause epithelial-myofibroblast transdifferentiation via the receptor for advanced glycation end products (RAGE). *J. Clin. Invest.* **108**:1853–1863. doi:10.1172/JCI200111951.
55. Yoganathan, N., et al. 2002. Integrin-linked kinase, a promising cancer therapeutic target: biochemical and biological properties. *Pharmacol. Ther.* **93**:233–242.